Eur. Phys. J. D **4**, 109–123 (1998)

THE EUROPEAN PHYSICAL JOURNAL D

Photon statistics of a bad-cavity laser near threshold

S. Gnutzmann[a]

Fachbereich Physik, Universität GH Essen, 45117 Essen, Germany

Received: 13 November 1998 / Revised: 19 May 1998 / Accepted: 6 July 1998

Abstract. A simple model of a bad-cavity laser is presented based on Haken's master equation for N pumped two-level atoms in a cavity. *Via* adiabatic elimination of fast variables the whole photon statistics is solved analytically near threshold. It is shown that the second order coherence function $g^{(2)}(0)$ has a very different behavior near threshold for a bad-cavity laser compared to a good-cavity laser. The power spectrum illustrates nicely the different time scales involved in the dynamics.

PACS. 42.50.Ar Photon statistics and coherence theory – 42.55.Ah General laser theory

1 Introduction

The theoretical investigation of laser models had its high time about 25 years ago with important contributions by Lax, Louisell, Scully, Lamb, Weidlich and Haken and many others [1–4]. The so-called bad-cavity limit has become interesting in recent years in the investigation of micro lasers and future quantum-dot or quantum-well lasers. First experiments [5] and a thorough theoretical investigation [6] have set in. Here a simple model for a bad-cavity laser is presented that shows some of the main differences in the photon statistics and in the laser linewidth to the well-known good-cavity results. A simple model for a single-mode laser takes into account five degrees of freedom: one mode of the electromagnetic field (amplitude and phase), the macroscopic inversion and the macroscopic polarization (amplitude and phase). There is a typical time scale for each of these degrees of freedom connected to damping constants: $\tau_F = 1/\kappa$ for the electromagnetic field, $\tau_P = 1/\gamma_P$ for the polarization, and $\tau_I = 1/\gamma_I$ for the inversion. One may divide single-mode lasers in four classes [6] according to the relation between these damping constants:

1. $\gamma_P, \gamma_I \gg \kappa$ – dye laser, for example,
2. $\gamma_P \gg \kappa \sim \gamma_I$ – helium-neon, argon-ion,
3. $\gamma_P \gg \kappa \gg \gamma_I$ – ruby, semiconductor, Nd:YAG,
4. $\kappa \gg \gamma_P, \gamma_I$ – near-infrared noble-gas lasers and many far-infrared lasers.

Bad-cavity lasers constitute the fourth class.

The author presents an investigation based on Haken's master equation for N incoherently pumped two-level atoms in a cavity which are coupled to a single mode of the field. The time-scale separation $\kappa \gg \gamma_I, \gamma_P$ gives rise to a fast decay of the mode to an adiabatic equilibrium with the atomic variables. After this fast decay the mode follows the slow dynamics of the atoms adiabatically. By adiabatic elimination of the mode the author arrives at a Fokker-Planck equation for the macroscopic atomic variables which is valid for a large number of atoms in a bad cavity. A very similar approach has been done by Lugiato *et al.* [7] for the absorptive optical bistability to obtain the fluorescent spectrum and photon statistics. In this investigation the main concern will be the steady state photon number distribution near threshold. *Via* further adiabatic elimination this may be obtained analytically for some relevant limits of the parameters. Above threshold an exhaustive investigation of the bad-cavity limit has been done by Kolobov *et al.* [6] who have given analytic results for amplitude and phase fluctuations. The author tries in this work to regain some of their results with a much simpler model. This simplification makes an investigation near threshold possible, however some important effects have to be neglected (*e.g.* spontaneous decay of the atoms to other levels). The role of pumping statistics for the noise in laser output has been pointed out by many authors [6,8] and different noise reduction mechanisms have been suggested [9]. The author limits himself to Poissonian pumping statistics in this work being aware that regular pumping might change some of the results. For the lasers used in experiments [5] surely Poissonian pumping should be assumed. However many effects are neglected in this investigation that may play a role for photon statistics of a real bad-cavity laser in experiment.

The paper is organized as follows. After introducing Haken's laser model in Section 2 the mode is eliminated adiabatically in the bad-cavity limit in Section 3. A Gaussian approximation is made in Section 4 which is valid above threshold. The second-order coherence and the linewidth are discussed in this approximation. In Section 5 the conditions for a time-scale separation between the dynamics of the polarization and the inversion are investigated. If these conditions are satisfied the fast variable

[a] e-mail: sven.gnutzmann@uni-essen.de

may adiabatically eliminated and we remain with one single degree of freedom ruling the dynamics. The conditions for time-scale separation are often satisfied near threshold. In Section 6 the adiabatic elimination of fast variables near threshold is carried out. The total photon-number distribution is derived analytically and the second-order coherence $g^{(2)}(0)$ is discussed and compared to the results of the Gaussian approximation. The dynamical behavior of fluctuations is discussed in Section 7 where the second-order coherence $g^{(2)}(t)$ and its Fourier transform the power spectrum $S(\omega)$ are computed numerically in the adiabatic elimination regime and an analytical expression is given for the Gaussian approximation which is valid above threshold.

2 Haken's laser model

We consider N effective two level atoms inside a cavity coupled to one mode of the electromagnetic field. Each atom is damped independently by its own heat bath and pumped incoherently. The time evolution of the statistical operator of the N atoms and the resonator mode are described by Haken's master equation [1,4]

$$\frac{\partial}{\partial t}\rho = \frac{1}{i\hbar}\left[H_{AF},\rho\right] + \Lambda_F\rho + \Lambda_A\rho. \tag{2.1}$$

The interaction Hamiltonian in dipole and rotating-wave approximation is

$$H_{AF} = i\hbar g\left(J_- b^\dagger - J_+ b\right) \tag{2.2}$$

where $b, b^\dagger$ are the creation and annihilation operators of the resonator mode and $J_\pm = \sum_{i=1}^N \sigma_\pm$ are the operators of the macroscopic polarization of the atoms. The first damping term $\Lambda_{F\rho}$ describes the damping of the mode due to losses through the mirrors. It is given by the well-known quantum optical master equation [1–3,10–12]

$$\Lambda_F\rho = \kappa\left(\left[b,\rho b^\dagger\right] + \left[b\,\rho, b^\dagger\right]\right). \tag{2.3}$$

Damping and pumping of the atoms is described by independent heat baths for each atom $\Lambda_A\rho = \sum_{i=1}^N \Lambda_i\rho$ and where Λ_i is the damping generator for one atom [1,10–12]

$$\begin{aligned}\Lambda_i\rho = {}& \frac{\gamma_I}{4}(1-2\sigma_0)\left(\left[\sigma^-,\rho\,\sigma^+\right] + \left[\sigma^-\,\rho,\sigma^+\right]\right)\\ &+ \frac{\gamma_I}{4}(1+2\sigma_0)\left(\left[\sigma^+,\rho\,\sigma^-\right] + \left[\sigma^+\,\rho,\sigma^-\right]\right)\\ &+ \left(\gamma_P - \frac{\gamma_I}{2}\right)\left(\left[\sigma^z,\rho\,\sigma^z\right] + \left[\sigma^z\,\rho,\sigma^z\right]\right).\end{aligned} \tag{2.4}$$

Here the σ^+,σ^- levels of the atom. The two damping constants γ_I and γ_P are constrained by $\gamma_I \le 2\gamma_P$. Equality holds when there are no phase destroying processes [1]. The last constant in equation (2.4) to be explained is the so called unsaturated inversion σ_0 which is the equilibrium value of the inversion $\langle\sigma^z\rangle_{equ} = \sigma_0$ of one atom if there is no coupling to the mode ($g = 0$). This parameter ranges in $-1/2 \le \sigma_0 \le 1/2$ and describes the pump strength. Apart from rotating-wave and dipole approximation weak coupling $g \ll \gamma_I, \gamma_P, \kappa$ has to be assumed in (2.1).

2.1 Pumping mechanism

Relatively recently it was shown by many authors that the fluctuations of the pumping mechanism play a central role in laser photon statistics [6,8]. These investigations assume that inverted atoms are shot into a cavity and start to interact with the cavity mode. The pumping mechanism is described by a mean rate R (giving the mean number of atoms arriving in the cavity per unit of time) and the statistics of arrival times which may be Poissonian if arrival times are assumed to be uncorrelated, regular if the nth atom arrives at the time $t_n = t_0 + n\frac{1}{R}$, or anything between these extremes. In the Haken model of the laser no atoms are shot into the cavity and the number of atoms is fixed. Still one can relate the rate R to the unsaturated inversion by

$$R = \gamma_I \frac{1+2\sigma_0}{1-2\sigma_0}\,. \tag{2.5}$$

As every atom in the Haken model is pumped and damped independently the excitation of one atom by the pumping mechanism is not correlated to the excitation of other atoms – the pumping statistics in the Haken model should be assumed to be of Poissonian type.

2.2 Changing to a c-number representation

The master equation (2.1) contains information about every individual atom, much more than needed. It can be shown [1] that all information about collective atom operators and the mode are described by a generalized Fokker-Planck equation for a quasi-probability distribution $P(\beta,\beta^\star,s,s^\star,s_z;t)$ where the operators have been associated with c-numbers according to

$$\begin{aligned} J_-, J_+ &\longleftrightarrow s, s^\star\\ J_z &\longleftrightarrow s_z\\ b, b^\dagger &\longleftrightarrow \beta, \beta^\star. \end{aligned} \tag{2.6}$$

Expectation values of the operators are connected to the corresponding expectation values of the c-numbers by a prescribed ordering of the operators

$$\begin{aligned}&\langle J_+^p J_z^q J_-^r b^{\dagger s} b^t\rangle =\\ &\int d^2\beta d^2 s ds_z\; s^{\star p} s^q s_z^r b^{\star s} b^t\; P(\beta,\beta^\star,s,s^\star,s_z;t).\end{aligned} \tag{2.7}$$

The evolution equation for the quasi-probability distribution P contains arbitrarily high derivatives. It reads

$$\begin{aligned}&\frac{\partial}{\partial t}\,P(\beta,\beta^\star,s,s^\star,s_z;t) =\\ &\left[L_A + L_F + L_{AF}\right]\,P(\beta,\beta^\star,s,s^\star,s_z;t)\end{aligned} \tag{2.8}$$

where the generators are given by

$$\begin{aligned}L_A = &\frac{\gamma_I}{4}(1-2\sigma_0)\\ &\times\left[\frac{\partial}{\partial s}s+\frac{\partial}{\partial s^\star}s^\star+\left(\exp\left(\frac{\partial}{\partial s_z}\right)-1\right)(N+2s_z)\right]\\ &+\frac{\gamma_I}{4}(1+2\sigma_0)\left[\frac{\partial}{\partial s}s+\frac{\partial}{\partial s^\star}s^\star+\left(\exp\left(-\frac{\partial}{\partial s_z}\right)-1\right)(N-2s_z)\right.\\ &+2N\frac{\partial^2}{\partial s\partial s^\star}+2\left(\exp\left(-\frac{\partial}{\partial s_z}\right)-1\right)\left(\frac{\partial}{\partial s}s+\frac{\partial}{\partial s^\star}s^\star\right)\\ &\left.+2\frac{\partial^2}{\partial s\partial s^\star}\left(\frac{\partial}{\partial s}s+\frac{\partial}{\partial s^\star}s^\star\right)+\frac{\partial^4}{\partial s^2\partial s^{\star\,2}}\exp\left(\frac{\partial}{\partial s_z}\right)(N+2s_z)\right]\\ &+\left(\gamma_P-\frac{\gamma_I}{2}\right)\left[\frac{\partial^2}{\partial s\partial s^\star}\exp\left(\frac{\partial}{\partial s_z}\right)(N+2s_z)+\frac{\partial}{\partial s}s+\frac{\partial}{\partial s^\star}s^\star\right]\end{aligned} \tag{2.9}$$

$$L_F=\kappa\left[\frac{\partial}{\partial\beta}\beta+\frac{\partial}{\partial\beta^\star}\beta\star\right] \tag{2.10}$$

$$\begin{aligned}L_{AF}=g\Big[&-\frac{\partial}{\partial\beta}s-\frac{\partial}{\partial\beta^\star}s^\star-\left(\exp\left(-\frac{\partial}{\partial s_z}\right)-1\right)(\beta s^\star+\beta^\star s)\\ &-2s_z\left(\frac{\partial}{\partial s}\beta+\frac{\partial}{\partial s^\star}\beta^\star\right)+\frac{\partial^2}{\partial s^2}s\beta+\frac{\partial^2}{\partial s^{\star\,2}}s^\star\beta^\star\Big].\end{aligned} \tag{2.11}$$

The generalized Fokker-Planck equation (2.8) is the starting point of this investigation [13]. The deterministic part which includes only first-order derivatives yields for the unsaturated inversion σ_0 a critical value σ_c the so-called critical inversion

$$\sigma_c=\frac{\kappa\gamma_P}{2Ng^2}\,. \tag{2.12}$$

For weak pumping, $\sigma_0<\sigma_c$, the resonator mode is not excited while above threshold, $\sigma_0>\sigma_c$, the equilibrium photon number of the mode increases linearly with the unsaturated inversion σ_0. Due to the weak coupling we have assumed in (2.1) we have

$$N\sigma_c=\frac{\kappa\gamma_P}{2g^2}\gg 1. \tag{2.13}$$

3 Bad-cavity limit

The dynamics of the model presented depends on the relative magnitude of the the damping constants γ_I,γ_P and κ and the coupling constant g. In many lasers there is a time scale separation such that the atoms relax to an adiabatic equilibrium much faster than the resonator mode, hence $\gamma_I,\gamma_P\gg\kappa$. Then the atomic dynamics may be eliminated adiabatically as done by Risken [1,14] who has discussed this case exhaustively. He derives a master equation for the mode with the dynamics of a van-der-Pol oscillator. Lately the opposite time-scale separation has become of interest which is known as the bad-cavity limit $\kappa\gg\gamma_I,\gamma_P$. In that case we may adiabatically eliminate the resonator mode. The remaining dynamics will depend only on atomic variables. The formalism of adiabatic elimination as used several times in this work is given in [15–17]. We are interested only in the slow dynamics of the atoms and assume the mode always to be in adiabatic equilibrium to the atoms, *i.e.* the quasi-probability distribution P is approximated by

$$P(\beta,\beta^\star,s,s^\star,s_z;t)=P_{ad}(\beta,\beta^\star|s,s^\star,s_z)P_{red}(s,s^\star,s_z;t) \tag{3.1}$$

where P_{ad} describes the adiabatic equilibrium of the mode with respect to given values for the atomic variables and P_{red} is the reduced quasi-probability density of the atomic variables,

$$P_{red}(s,s^\star,s_z;t)\;=\;\int d^2\beta\,P(\beta,\beta^\star,s,s^\star,s_z;t). \tag{3.2}$$

The adiabatic equilibrium is determined by

$$\left[\frac{\partial}{\partial\beta}(\kappa\,\beta-g\,s)+\frac{\partial}{\partial\beta^\star}(\kappa\,\beta^\star-gs^\star)\right]P_{ad}(\beta,\beta^\star|s,s^\star,s_z)=0 \tag{3.3}$$

which takes into account that part of the interaction which depends on the atomic variables only parametrically. This leads to a delta-peaked distribution

$$P_{ad}(\beta,\beta^\star|s,s^\star)=\delta^2(\beta-\frac{g}{\kappa}s). \tag{3.4}$$

Thus the resonator mode has the same statistics as the atomic polarization in the sense

$$\langle\beta^m\beta^{\star n}\rangle=\left(\frac{g}{\kappa}\right)^{m+n}\langle s^m s^{\star\,n}\rangle. \tag{3.5}$$

The reduced dynamics is given by the generalized Fokker-Planck equation

$$\frac{\partial}{\partial t}P_{red}(s,s^\star,s_z;t)=LP_{red}(s,s^\star,s_z;t) \tag{3.6}$$

with

$$\begin{aligned}L=L_A+&\frac{2g^2}{\kappa}\\ &\times\left[\left(1-\exp\left(-\frac{\partial}{\partial s_z}\right)\right)ss^\star-\left(\frac{\partial}{\partial s}s+\frac{\partial}{\partial s^\star}s^\star\right)s_z\right.\\ &\left.+\frac{1}{2}\left(\frac{\partial^2}{\partial s^2}s^2+\frac{\partial^2}{\partial s^{\star\,2}}s^{\star\,2}\right)\right].\end{aligned} \tag{3.7}$$

This is still a very unhandy equation for calculations with its infinitely high derivatives even if we are interested only in steady state solutions. However, we can simplify this equation considerably by truncating all higher derivatives than second-order ones. In order to give a self-consistent argument why this truncation is trustworthy we refer to a result that will be obtained in the following sections with the truncated Fokker-Planck equation. It will be shown that the threshold values at $\sigma_0=\sigma_c$ of the polarization and the inversion are given by

$$r_c=\langle s^\star s\rangle=N\sigma_c\sqrt{N\frac{\gamma_I}{2\gamma_P}} \tag{3.8}$$

$$N\sigma_c-z_c=\;\langle s_z\rangle\;=N\sigma_c-\sqrt{N\frac{\gamma_P}{2\gamma_I}}. \tag{3.9}$$

We may introduce reduced variables $S, S^\star$ and z

$$\begin{aligned} s &= S\sqrt{r_c} \\ s^\star &= S^\star\sqrt{r_c} \\ s_z &= N\sigma_c + z\, z_c \end{aligned} \tag{3.10}$$

such that near threshold the magnitudes of the dimensionless reduced variables are of the order of one. Upon using

$$N \gg N\sigma_c \gg 1,\ |\sigma_0| \ll 1 \tag{3.11}$$

we may simplify the generator L given by (3.7) to

$$\begin{aligned} L = \gamma_P \Bigg\{ &-\frac{N}{2r_c}\left[\frac{\partial}{\partial S}S + \frac{\partial}{\partial S^\star}S^\star\right] z + \frac{N}{2z_c^2}\frac{\partial}{\partial z}\left[z - p + S^\star S\right] \\ &+ \frac{N}{r_c}\frac{\partial^2}{\partial S \partial S^\star} + \frac{N^2}{8z_c^4}\frac{\partial^2}{\partial z^2}\Bigg\} + \mathcal{O}\left(\sqrt{\frac{1}{N}}, \frac{1}{N\sigma_c}\right). \end{aligned} \tag{3.12}$$

A new parameter p has been introduced in the first line of (3.12) which replaces the unsaturated inversion and will be called pump strength further on

$$p = \sqrt{\frac{2N\gamma_I}{\gamma_P}}\left(\sigma_0 - \sigma_c\right). \tag{3.13}$$

The threshold appears at $p = 0$. It will be convenient to employ polar coordinates for the polarization

$$\begin{aligned} S &= \sqrt{r}\exp(i\phi) \\ r &= S^\star S \end{aligned} \tag{3.14}$$

and to rescale the time

$$t \longrightarrow \tilde{t} = \frac{\gamma_P N}{r_c} t. \tag{3.15}$$

We arrive at the generator

$$L = L_r + L_\phi \tag{3.16}$$

$$\begin{aligned} L_r = &-\frac{\partial}{\partial r}\left[rz + 1\right] + \alpha\frac{\partial}{\partial z}\left[z - p + r\right] \\ &+ \frac{\partial^2}{\partial r^2}r + \alpha\frac{\gamma_I}{2\gamma_P}\frac{\partial^2}{\partial z^2} \end{aligned} \tag{3.17}$$

$$L_\phi = \frac{1}{4}\frac{\partial^2}{\partial\phi^2}\frac{1}{r} \tag{3.18}$$

where

$$\begin{aligned} \alpha &= \frac{r_c}{2z_c^2} \\ &= \sqrt{\frac{\kappa^2\gamma_I^3}{8Ng^4\gamma_P}}. \end{aligned} \tag{3.19}$$

With the generators (3.16–3.18) the Fokker-Planck equation (3.6) contains all important information about the system in steady state. Further adiabatic eliminations of either the polarization intensity r or the reduced inversion z may be carried out in certain limits (Sects. 5 and 6). The steady state quasi-probability distribution P_{stat} does not depend on the phase ϕ and is a solution to

$$L_r P_{stat}(r, z) = 0. \tag{3.20}$$

The phase-diffusion part L_ϕ will be taken into account only when we are discussing the laser linewidth in Section 4.3.

4 Gaussian approximation

The Gaussian approximation consists in first solving the deterministic part of the Fokker-Planck equation (3.6) and treat the fluctuations around this dynamics represented by the second order derivatives as small perturbations. Using radial coordinates is of great advantage here, first because of the symmetry and second because the net force of the thermal fluctuations (due to the coupling of the atoms to some pumping reservoir) on the intensity of the polarization shows up in the deterministic part (the term $-\frac{\partial}{\partial r}$ in the first line of (3.17)). This approximation is surely good well above threshold and it will show to be of some value even near threshold. Due to the inclusion of the net force of thermal fluctuations in the drift first moments are treated correctly near threshold. High above threshold however this net force may justly be neglected without much influence on the first moments.

4.1 Deterministic dynamics

The deterministic part of the Fokker-Planck equation is obtained by taking into account only the drift terms in (3.17). The mean reduced inversion and the mean polarization are then described by deterministic equations (writing r_0 instead of $\langle r\rangle$)

$$\begin{aligned} \frac{d}{d\tilde{t}}r_0 &= r_0 z_0 + 1 \\ \frac{d}{d\tilde{t}}z_0 &= \alpha\left[p - z_0 - r_0\right]. \end{aligned} \tag{4.1}$$

The steady state of the reduced inversion and the polarization is reached at

$$\begin{aligned} r_0 &= \frac{p}{2} + \sqrt{\frac{p^2}{4} + 1} \\ z_0 &= \frac{p}{2} - \sqrt{\frac{p^2}{4} + 1}. \end{aligned} \tag{4.2}$$

Far below and far above threshold, $|p| \gg 1$, these solutions are linear in the pump strength. Far below threshold the mean polarization intensity r_0 is almost zero and the mean reduced inversion z_0 increases with p. Far above threshold the intensity increases and the reduced inversion is almost zero. Near threshold $p \approx 1$ the action of the net force of fluctuations is responsible for the smooth connection of the linear parts (see Figs. 1, 2).

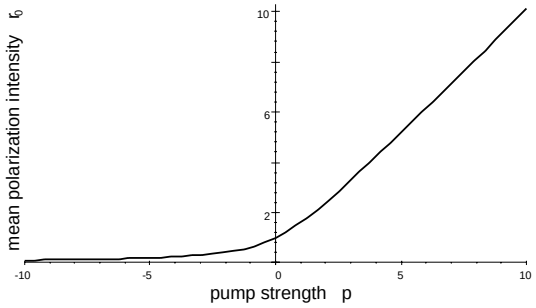

Fig. 1. Mean polarization intensity in Gaussian approximation as a function of the pump strength p (proportional to the mean photon number).

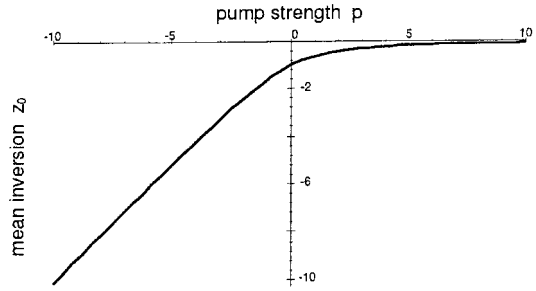

Fig. 2. Mean reduced inversion in Gaussian approximation as a function of the pump strength p.

4.2 Fluctuations of the photon number

Assuming that the steady state quasi-probability distribution $P(r,z)$ which solves (3.20) will be peaked around the steady state solution (4.2) of the deterministic dynamics we may linearize (3.17). We set

$$\begin{aligned} r &= r_0 + \Delta r \\ z &= z_0 + \Delta z, \end{aligned} \tag{4.3}$$

where r_0 and z_0 are given by (4.2). The new variables Δr and Δz are considered as small numbers. After transforming the generator L_r given by (3.17) to the new variables we keep only the lowest nonvanishing powers. The linearized generator found in this way is given by

$$\begin{aligned} L_{r,lin} = &\frac{\partial}{\partial \Delta r}\left[\frac{1}{r_0}\Delta r - r_0 \Delta z\right] \\ &+\alpha \frac{\partial}{\partial \Delta z}\left[\Delta z + \Delta r\right] \\ &+\frac{\partial^2}{\partial \Delta r^2} r_0 + \alpha \frac{\gamma_I}{2\gamma_P}\frac{\partial^2}{\partial \Delta z^2}. \end{aligned} \tag{4.4}$$

This leads to a steady-state distribution $P(r = r_0 + \Delta r, z = z_0 + \Delta z)$ which is given by a Gaussian centered at $r = r_0, z = z_0$ with second moments

$$\begin{aligned} \langle \Delta r \Delta z\rangle_0 &= \frac{r_0^2\left(\frac{\gamma_I}{2\gamma_P} - \alpha r_0\right)}{r_0^2 + 1 + \alpha\left(r_0 + r_0^3\right)} \\ \langle \Delta r^2\rangle_0 &= r_0^2\left(\langle \Delta r \Delta z\rangle_0 + 1\right) \\ \langle \Delta z^2\rangle_0 &= \langle \Delta r \Delta z\rangle_0 + \frac{\gamma_I}{\gamma_P}. \end{aligned} \tag{4.5}$$

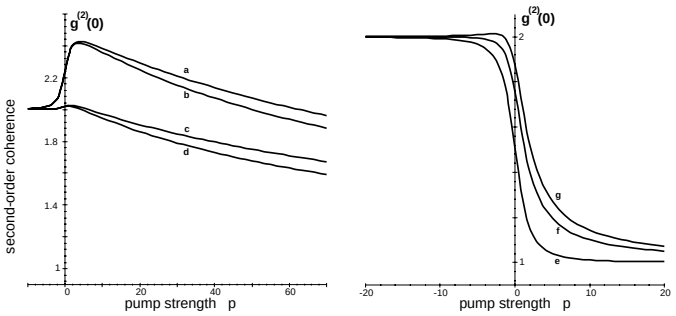

Fig. 3. Second-order correlation function $g^{(2)}(0)$ in Gaussian approximation as a function of the pump strength p for some values of the parameters $\frac{2\gamma_P}{\gamma_I}$ and α: (a) $\frac{2\gamma_P}{\gamma_I} = 2$, $\alpha = 0.008$; (b) 2, 0.01; (c) 20, 0.008; (d) 20, 0.01; (e) 2, 100; (f) 50, 1; (g) 2, 1.

The photon statistics may be characterized by the second-order correlation function [11,18]

$$\begin{aligned} g^{(2)}(0) &= \frac{\langle b^\dagger b^\dagger b b\rangle}{\langle b^\dagger b\rangle^2} \\ &= 1 + \frac{\mathrm{Var}\left(b^\dagger b\right) - \langle b^\dagger b\rangle}{\langle b^\dagger b\rangle^2} \\ &= \frac{\langle r^2\rangle}{\langle r\rangle^2}. \end{aligned} \tag{4.6}$$

The last equality is due to the equivalence of the quasi-probability distribution used here to the so called P-function. The moments of the P-function are equal to the normally ordered moments of the photon creation and annihilation operators. This second-order correlation $g^{(2)}(0)$ is defined in such a way that it gives $g^{(2)}(0) = 1$ for a Poissonian photon-number distribution like in a coherent state. A Poissonian distribution has $\mathrm{Var}\left(b^\dagger b\right) = \langle b^\dagger b\rangle$. The photon statistics is called sub-Poissonian if $g^{(2)}(0) < 1$ and super-Poissonian for $g^{(2)}(0) > 1$. In a thermal state $g^{(2)}(0) = 2$. In the Gaussian approximation made in this section the correlation function is given by

$$g^{(2)}(0) = 2 + \langle \Delta r \Delta z\rangle_0. \tag{4.7}$$

In Figure 3 the correlation function is plotted as a function of the pump strength p for some values of the two parameters $\frac{\gamma_I}{2\gamma_P}$ and $\frac{r_c}{2z_c^2}$. Well below threshold the photon statistics has thermal character $g^{(2)}(0) = 2$ for any value of the parameters. The behavior of the second-order correlation near and above threshold strongly depends on the parameter $\alpha = \frac{r_c}{2z_c^2}$. For large values $\alpha \gg 1$ there is a fast transition to Poissonian statistics near threshold. This is the same behavior as is shown by Risken's master equation with the dynamics of a van-der-Pol oscillator [1,14,19]. However for small values $\alpha \ll 1$ a very different and new behavior is seen. Near threshold the second-order correlation does not show a fast decay but may even rise.

Well above threshold $p \gg 1$ there is still a transition to Poissonian statistics, but the decay of $g^{(2)}(0)$ to one is only proportional to $1/p$ so that even well above threshold super-Poissonian statistics may be observed. This Gaussian approximation is surely not strictly satisfactory near threshold where the neglected part in the deterministic part of the Fokker-Planck equation (4.4) is of the same order of magnitude as the terms kept. Well above or below threshold $|p| \gg 1$ the solution is self-consistent and we will see in the following treatment (Sect. 6) that even near threshold this Gaussian approximation has the right qualitative behavior.

4.3 Linewidth of the laser

The linewidth $\Delta\nu$ of the laser above threshold is connected to the phase-diffusion generator

$$L_\phi = \frac{1}{2} D_\phi \frac{\partial^2}{\partial \phi^2} \tag{4.8}$$

given by (3.18). This phase diffusion sets the time scale on which an initially prescribed phase is destroyed. The linewidth $\Delta\nu$ is given by the inverse of this time scale:

$$\begin{aligned} \Delta\nu &= \frac{\partial \tilde{t}}{\partial t} D_\phi \\ &= \frac{N}{2} \frac{\gamma_P g^2}{\kappa^2 \mathcal{I}}, \end{aligned} \tag{4.9}$$

where $\mathcal{I}$ is the photon number inside the cavity

$$\mathcal{I} = \frac{g^2}{\kappa^2} r_c r. \tag{4.10}$$

This result is in agreement with the result of [5,6]. The phase diffusion of a bad-cavity laser is seen to be reduced by a factor $\frac{\gamma_P^2}{\kappa^2} \ll 1$ in comparison to the Schawlow-Townes result [3,20] valid for good cavities given by

$$\Delta\nu_{ST} = \frac{N}{2} \frac{g^2}{\gamma_P \mathcal{I}}\,. \tag{4.11}$$

5 Time-scale separation near threshold

In this section the time-scale separation in the dynamics between the polarization intensity r and the reduced inversion z is studied in order to give the conditions for further adiabatic elimination of fast variables from the Fokker-Planck equation (3.6). After eliminating the resonator mode assuming $\kappa \gg \gamma_I, \gamma_P$ one would think that the time-scale separation between the dynamics of the polarization and of the inversion is determined from the relation between their damping constants γ_P and γ_I. However due to the nonlinear coupling in this laser model it is a bit more complicated. We have to look closer at the deterministic equations (4.1) to investigate the time-scale separation. There are just two parameters that may determine the time scales of the dynamics: the pump strength p and the ratio $\alpha = r_c/(2z_c^2)$ By a first estimate on account of the deterministic equations the typical inverse time scale for the dynamics of the reduced inversion z is given by α whereas the typical inverse time scale for the polarization r is given by equilibrium value of the reduced inversion z_0 which depends on the pump strength p (we are interested only in the dynamics very near steady state here). So above threshold when z tends to zero the polarization intensity slows down. More strictly the time scales may be derived by looking at the short time behavior of the deterministic dynamics given by the linearized version of (4.1)

$$\begin{aligned} \frac{d}{d\tilde{t}} \delta r(\tilde{t}) &= z_0 \delta r(\tilde{t}) + r_0 \delta z(\tilde{t}) + r_0 z_0 + 1 \\ \frac{d}{d\tilde{t}} \delta z(\tilde{t}) &= \alpha \left(+ [p - z_0 - r_0] - \delta r(\tilde{t}) - \delta z(\tilde{t}) \right), \end{aligned} \tag{5.1}$$

where we have written $r_0(t) = r_0 + \delta r(t)$ and $z_0(t) = z_0 + \delta r(t)$ and have neglected higher orders of δ. The constants r_0 and z_0 have arbitrary values here (not necessarily the steady state solutions of the deterministic dynamics). The typical inverse time scales of the dynamics near r_0 and z_0 are given by the eigenvalues of the homogeneous part

$$\lambda_\pm = -\frac{\alpha - z_0}{2} \pm \sqrt{\left(\frac{\alpha - z_0}{2}\right)^2 - \alpha\,(r_0 - z_0)}. \tag{5.2}$$

As a condition for time-scale separation the square root in these eigenvalues must be real

$$\frac{r_0}{\alpha} < \frac{1}{4} \left(1 + \frac{z_0}{\alpha}\right)^2. \tag{5.3}$$

Now we assume that the steady state distribution of the full Fokker-Planck equation (3.17) is peaked around the equilibrium point of the deterministic dynamics given by (4.2) in such a way that the eigenvalues $\lambda_\pm$ do not change within the width of the distribution. Around these steady states the inverse time scales are given by setting $z_0 = -\frac{1}{r_0}$ in (5.2).

$$\lambda_\pm = \frac{1}{2} \left(-\alpha - \frac{1}{r_0} \pm \sqrt{(\alpha - \frac{1}{r_0})^2 - 4\alpha r_0} \right). \tag{5.4}$$

In Figure 4 the contours of $\lambda_-/\lambda_+ = const$ are shown to illustrate the regions in the space spanned by r and z where there is a time-scale separation. The two graphs shown there are plotted in scaled variables r/α and z/α. Above the thick contour ($\lambda_-/\lambda_+ = 1$) the condition (5.3) for the two eigenvalues $\lambda_\pm$ does not hold. There is no time-scale separation in this region. By looking on these inverse time scales it can be seen that well below threshold $r_0 \ll 0$ there will always be a good time-scale separation whereas well above threshold the two inverse time scales become complex conjugate of one another. Near threshold

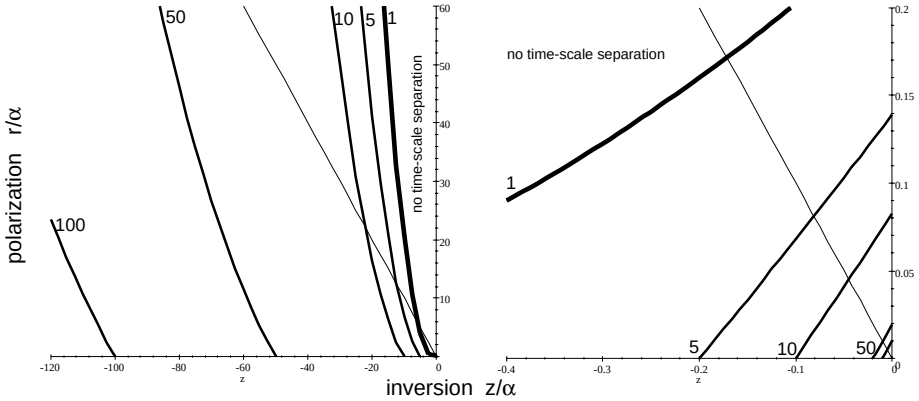

Fig. 4. Illustration of time-scale separation. The two graphs show the contours of $|\frac{\lambda_-}{\lambda_+}| = const$ for $const = 1, 5, 10, 50, 100$ in rescaled variables r/α and z/α. The right graph is a magnification of the region near the origin. The thick curve with $const = 1$ separates the region of space where $\lambda_\pm$ become complex conjugate of one another. The thin line gives the mean values of the polarization intensity and the reduced inversion at threshold in the Gaussian approximation (that is $r_0 = 1, z_0 = -1$) for arbitrary value of α.

$r \approx 1$ we have time scale separation when either $\alpha \ll 1/10$ or when $\alpha \gg 10$. It may be shown that the variable connected to fast decay to equilibrium is the polarization r for $\alpha \ll 1/10$ whereas for $\alpha \gg 10$ the reduced inversion z is the fast variable. In these cases we may carry out a further adiabatic elimination to arrive at a Fokker-Planck equation in one single variable which is always solvable analytically.

6 Adiabatic elimination of fast variables near threshold

If the condition for time-scale separation near threshold given in the last section $\alpha \ll 1/10$ or $\alpha \gg 10$ is satisfied our Fokker-Planck equation

$$\frac{\partial}{\partial \tilde{t}} P(r, z; \tilde{t}) = L_r P(r, z; \tilde{t}) \tag{6.1}$$

may be simplified considerably by adiabatic elimination of the fast variable. However dynamics will be treated consistently only for such distributions $P(r, z; \tilde{t})$ which are near the stationary distribution and are peaked around the steady state solution of the deterministic equations. In order to carry out the adiabatic elimination we separate the generator L_r into a part L_P which describes the polarization intensity and a second part L_I for the reduced inversion:

$$\begin{aligned} L_r &= L_P + L_I \\ L_P &= -\frac{\partial}{\partial r}\left[rz + 1\right] + \frac{\partial^2}{\partial r^2} r \qquad (6.2) \\ L_I &= \alpha \left[\frac{\partial}{\partial z}\left(z + r - p\right) + \frac{\gamma_I}{2\gamma_P}\frac{\partial^2}{\partial z^2}\right]. \qquad (6.3) \end{aligned}$$

We will treat the two cases of fast inversion and fast polarization separately and give the stationary distributions in both cases.

6.1 Fast inversion-slow polarization

If $\frac{r_c}{2z_c^2} \gg 10$ inversion is fast near threshold and may be eliminated adiabatically. We may assume that the polarization remains constant while inversion goes to its adiabatic equilibrium and may therefor write the quasi-probability distribution as product

$$P(r, z; \tilde{t}) = P_{ad}(z|r) P(r; \tilde{t}). \tag{6.4}$$

The adiabatic equilibrium $P_{ad}(z|r)$ with a given polarization r is determined by

$$L_I P_{ad}(z|r) = 0. \tag{6.5}$$

This gives a Gaussian distribution

$$P_{ad}(z|r) = \sqrt{\frac{\gamma_I}{\gamma_P}\pi} \exp\left(-\frac{\gamma_P}{\gamma_I}\left(z + r - p\right)^2\right) \tag{6.6}$$

with a mean value

$$\langle z \rangle_{ad}(r) = p - r. \tag{6.7}$$

The slow dynamics of the distribution of the polarization $P(r; \tilde{t})$ is to lowest order described by the reduced dynamics

$$\frac{\partial}{\partial \tilde{t}} P(r; \tilde{t}) = \ell_P P(r; \tilde{t}) \tag{6.8}$$

where the generator is ℓ_P is a averaged version of L_P (6.3)

$$\begin{aligned} \ell_P &= \int dz P_{ad}(z|r) L_P \\ &= -\frac{\partial}{\partial r}\left[r\left(p - r\right) + 1\right] + \frac{\partial^2}{\partial r^2} r. \qquad (6.9) \end{aligned}$$

This is the generator of a van-der-Pol oscillator. The generated dynamics is equivalent to the well-known one-mode

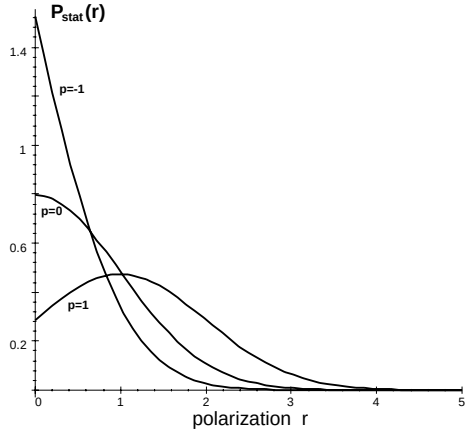

Fig. 5. Stationary probability distribution of the polarization intensity $P_{stat}(r)$ (proportional to photon number distribution) for slow polarization ($\alpha \gg 10$).

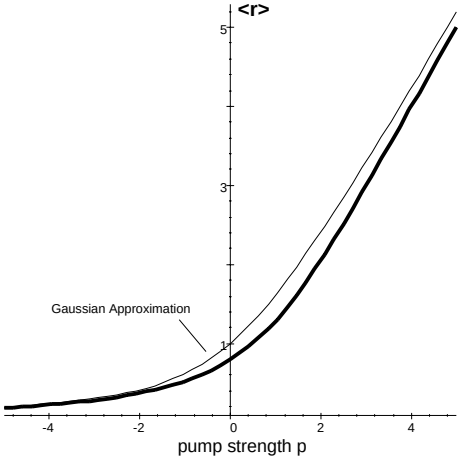

Fig. 6. Mean polarization intensity $\langle r\rangle$ (proportional to mean photon number) as a function of the pump strength p for slow polarization ($\alpha \gg 10$). The thin line gives the result of the Gaussian approximation.

laser in a good cavity. The stationary distribution is easily derived

$$P_{stat}(r) = \frac{1}{\mathcal{N}} \exp\left(-\frac{1}{2}(r-p)^2\right) \tag{6.10}$$

where the normalization is given by

$$\mathcal{N} = \sqrt{\frac{\pi}{2}}\left(1+\mathrm{erf}\left(\frac{p}{\sqrt{2}}\right)\right). \tag{6.11}$$

The stationary distribution $P_{stat}(r)$ is shown in Figure 5 for some values of the pump strength p near threshold. The polarization intensity r is connected to the photon number $\mathcal{I}$ by

$$\begin{aligned} \mathcal{I} &= \mathcal{I}_c r, \\ \mathcal{I}_c &= \frac{g^2}{\kappa^2} r_c = \frac{\gamma_P}{2\kappa}\sqrt{N\frac{\gamma_I}{2\gamma_P}}, \end{aligned} \tag{6.12}$$

so to get the photon number distribution we just have to rescale $P_{stat}(r)$ appropriately. The stationary distribution $P_{stat}(z)$ of the reduced inversion z is obtained by integration

$$\begin{aligned} P_{stat}(z) &= \int dr P_{ad}(z|r) P_{stat}(r) \\ &= C\left(1-\mathrm{erf}\left(\frac{\frac{2\gamma_P}{\gamma_I}(z-p)-p}{\sqrt{2\left(\frac{2\gamma_P}{\gamma_I}+1\right)}}\right)\right)\exp\left(-\frac{\gamma_P}{2\gamma_P+\gamma_I}z^2\right), \\ C &= \sqrt{\frac{\gamma_P}{\pi(2\gamma_P+\gamma_I)}}\frac{1}{\mathrm{erf}\left(\frac{p}{\sqrt{2}}\right)+1}. \end{aligned} \tag{6.13}$$

The mean polarization intensity, photon number and reduced inversion are easily derived from the distributions (6.10) and (6.13)

$$\begin{aligned} \langle r\rangle &= p + \frac{1}{\sqrt{\frac{\pi}{2}}\left(1+\mathrm{erf}\left(\frac{p}{\sqrt{2}}\right)\right)}\exp\left(-\frac{p^2}{2}\right) \\ \langle z\rangle &= p - \langle r\rangle \\ \langle b^\dagger b\rangle &= \mathcal{I}_c\langle r\rangle . \end{aligned} \tag{6.14}$$

In Figure 6 the mean polarization intensity $\langle r\rangle$ is plotted as a function of the pump strength. The deviation from the Gaussian approximation is seen to be 20 percent near threshold. The variations are also easily calculated

$$\begin{aligned} \mathrm{Var}\,(r) &= 1+\frac{p^2}{4}-\left(\langle r\rangle-\frac{p}{2}\right)^2 \\ \mathrm{Var}\,(z) &= \mathrm{Var}\,(r)+\frac{\gamma_I}{2\gamma_P} \\ \mathrm{Var}\left(b^\dagger b\right) &= \mathcal{I}_c^2\mathrm{Var}\,(r). \end{aligned} \tag{6.15}$$

In Figure 7 the second-order correlation function $g^{(2)}(0)$ is shown. Near threshold it shows the well-known behavior of a good-cavity laser, *i.e.* the dropping from the value $g^{(2)}(0)=2$ indicating thermal fluctuations of the photon number below threshold to $g^{(2)}(0)=1$ indicating Poisson statistics like a coherent state.

6.2 Fast polarization-slow inversion

Now we assume $\alpha \ll 1/10$ [21]. Near threshold the polarization intensity is then a fast variable that we eliminate adiabatically in the same way as the reduced inversion has been eliminated in the previous subsection. The quasi-probability distribution is approximated by a product

$$P(r,z;\tilde{t}) = P_{ad}(r|z)P(z;\tilde{t}). \tag{6.16}$$

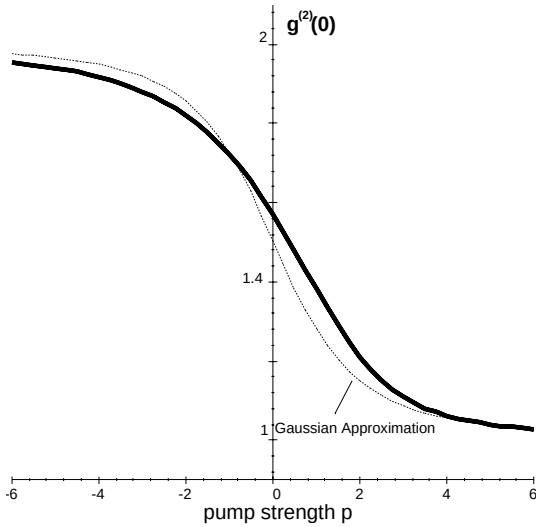

Fig. 7. Second-order correlation function $g^{(2)}(0)$ as a function of the pump strength p for slow polarization ($\alpha \gg 10$). The thin line gives the result of the Gaussian approximation.

and the adiabatic equilibrium of the polarization intensity with a given reduced inversion is determined by

$$L_P P_{ad}(r|z) = \left[-\frac{\partial}{\partial r}\left[rz+1\right] + \frac{\partial^2}{\partial r^2} r \right] P_{ad}(r|z) = 0. \tag{6.17}$$

If $z < 0$ this gives a Poisson distribution

$$P_{ad}(r|z) = -z \exp(zr), \tag{6.18}$$

with a mean given by

$$\langle r \rangle_{ad}(z) = -\frac{1}{z}\,. \tag{6.19}$$

For $z > 0$ however there is no normalizable distribution for the adiabatic equilibrium. As the dynamics of the reduced quasi-probability distribution $P(z;\tilde{t})$ is found by averaging over the adiabatic equilibrium for arbitrary z this seems to be inconsistent. This problem may be overcome by introducing an *ad-hoc* force in the generator L_P which regularizes the dynamics for $z > 0$

$$L_P(\epsilon) = \frac{\partial}{\partial r}\left[\epsilon r^2 - rz - 1\right] + \frac{\partial^2}{\partial r^2} r. \tag{6.20}$$

Taking the limit $\epsilon \longrightarrow 0$ in the end of all calculations is equivalent to restricting the dynamics to $z < 0$, setting $P(z) = 0$ for $z > 0$ and assigning the boundary condition $P(z = 0) = 0$. This is also natural as we expect $P(z)$ to be peaked around the deterministic solution (4.2) which is negative and assume $P(z)$ to have neglectable contributions where time-scale separation is not valid (see Sect. 5). Now we may proceed as in the last section for slow polarization. The reduced dynamics of the reduced inversion is in lowest order perturbation theory

$$\frac{\partial}{\partial \tilde{t}} P(r;\tilde{t}) = \ell_I P(r;\tilde{t}), \tag{6.21}$$

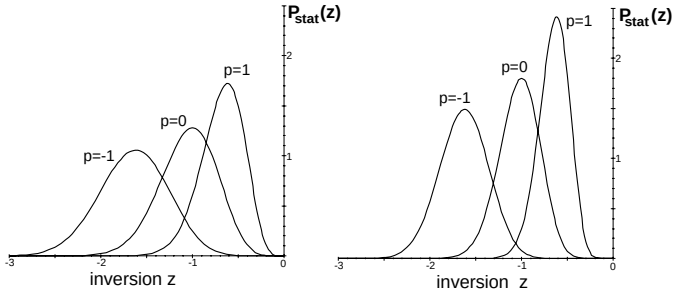

Fig. 8. Stationary probability distribution of the reduced inversion $P_{stat}(z)$ for slow inversion ($\alpha \ll 1/10$) for $2\gamma_P/\gamma_I = 5$ (left) and $2\gamma_P/\gamma_I = 10$ (right).

where the generator ℓ_I is given by L_P in (6.3) averaged over the adiabatic equilibrium $P_{ad}(r|z)$ (6.17)

$$\ell_I = \alpha \left[\frac{\partial}{\partial z}\left(z - \frac{1}{z} - p \right) + \frac{\gamma_I}{2\gamma_P} \frac{\partial^2}{\partial z^2} \right]. \tag{6.22}$$

The stationary distribution $P_{stat}(z)$ of the reduced inversion in this case is a product of a Gaussian with a power of z

$$P_{stat}(z) = \frac{1}{\mathcal{M}} (-z)^{\frac{2\gamma_P}{\gamma_I}} \exp\left(-\frac{\gamma_P}{\gamma_I} (z-p)^2 \right) \Theta(-z) \tag{6.23}$$

where $\mathcal{M}$ is the normalization constant

$$\mathcal{M} = \exp\left(-\frac{\gamma_P p^2}{\gamma_I}\right) \left(\frac{\gamma_P}{\gamma_I}\right)^{-\frac{2\gamma_P+\gamma_I}{2\gamma_I}} \times \sum_{m=0}^{\infty} \frac{1}{m!} \left(-\sqrt{\frac{\gamma_P}{\gamma_I}} p\right)^m \Gamma\left(\frac{\frac{2\gamma_P}{\gamma_I} + m + 1}{2}\right). \tag{6.24}$$

This function is shown in Figure 8. The stationary distribution of the polarization intensity $P_{stat}(r)$ is obtained by an integration

$$P_{stat}(r) = \int dz P_{ad}(r|z) P_{stat}(z). \tag{6.25}$$

The form of this function is shown in Figure 9. This is clearly not peaked around its mean so we will have to discuss if this is still self-consistent to the assumed time-scale separation. The moments of the polarization are connected to moments of $1/z$ by

$$\begin{aligned} \langle r^m \rangle &= \int_{-\infty}^{0} dz P_{stat}(z) \int_0^{\infty} dr (-z) r^m \exp(rz) \\ &= (-1)^m m! \langle z^{-m} \rangle. \end{aligned} \tag{6.26}$$

For $2\gamma_P = \gamma_I$ the moment $\langle r^2 \rangle = \langle z^{-2} \rangle$ diverges as may be seen from (6.23). In this case our approach may get

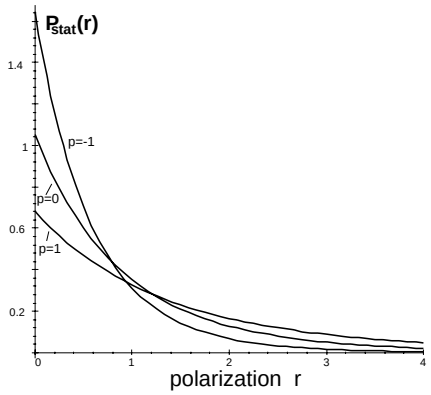

Fig. 9. Stationary probability distribution of the polarization intensity $P_{stat}(r)$ (proportional to photon number distribution) for slow inversion ($\alpha \ll 1/10$) for $2\gamma_P/\gamma_I = 5$.

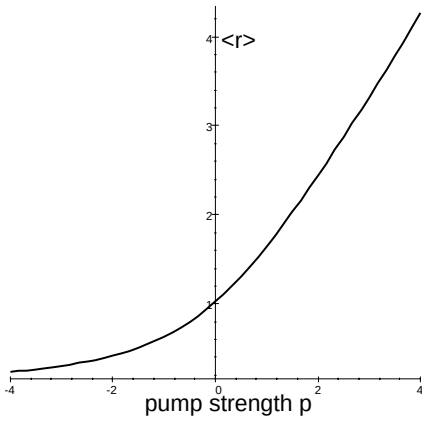

Fig. 10. Mean polarization intensity $\langle r\rangle$ (proportional to mean photon number) as a function of the pump strength p for slow inversion ($\alpha \ll 1/10$, here $2\gamma_P/\gamma_I = 5$). The result of the Gaussian approximation is very near the shown curve.

inconsistent and we have to assume a further condition $2\gamma_P \gg \gamma_I$ in order to have self-consistent results. Still only low order moments $\langle r^m\rangle$ with $m < \gamma_P/\gamma_I$ are surely treated correctly. The moments of the reduced inversion are given by the expression

$$\langle z^l\rangle = \left(-\sqrt{\frac{\gamma_I}{\gamma_P}}\right)^l \times \frac{\sum_{m=0}^{\infty}\left(-2p\sqrt{\frac{\gamma_P}{\gamma_I}}\right)^m \frac{\Gamma\left(\frac{1}{2}(\frac{2\gamma_P}{\gamma_I}+l+m+1)\right)}{\Gamma(m+1)}}{\sum_{n=0}^{\infty}\left(-2p\sqrt{\frac{\gamma_P}{\gamma_I}}\right)^n \frac{\Gamma\left(\frac{1}{2}(\frac{2\gamma_P}{\gamma_I}+n+1)\right)}{\Gamma(n+1)}} \tag{6.27}$$

where l may be any integer with

$$l > -\frac{2\gamma_P}{\gamma_I}\,. \tag{6.28}$$

The divergence of moments $\langle z^l\rangle$ for $l < -2\gamma_P/\gamma_I$ has its origin in the tail of the function $P_{stat}(z)$ near $z = 0$. Near $z = 0$ the assumed time-scale separation breaks down so that this tail of $P_{stat}(z)$ cannot be assumed to be treated correctly by our approach. The main weight of the function however is in a region where the time-scale separation holds and the approach is self-consistent. Only very high moments of the photon distribution depend on this artificial tail. At threshold the first moments simplify to

$$\begin{aligned}
\langle z\rangle_{thr} &= -\sqrt{\frac{\gamma_I}{\gamma_P}}\frac{\Gamma\left(\frac{\gamma_P}{\gamma_I}+1\right)}{\Gamma\left(\frac{\gamma_P}{\gamma_I}+\frac{1}{2}\right)} \\
&\simeq -1 \qquad \text{for } \frac{2\gamma_P}{\gamma_I} \gg 1 \\
\langle r\rangle_{thr} &= \sqrt{\frac{\gamma_P}{\gamma_I}}\frac{\Gamma\left(\frac{\gamma_P}{\gamma_I}\right)}{\Gamma\left(\frac{\gamma_P}{\gamma_I}+\frac{1}{2}\right)} \\
&\simeq 1 \qquad \text{for } \frac{2\gamma_P}{\gamma_I} \gg 1 \\
\langle z^2\rangle_{thr} &= \frac{2\gamma_P+\gamma_I}{2\gamma_P} \\
&\simeq 1 \qquad \text{for } \frac{2\gamma_P}{\gamma_I} \gg 1 \\
\langle r^2\rangle_{thr} &= 2\frac{2\gamma_P}{2\gamma_P-\gamma_I} \\
&\simeq 2 \qquad \text{for } \frac{2\gamma_P}{\gamma_I} \gg 1 \\
\mathrm{Var}\,(z) &\ll 1 \qquad \text{for } \frac{2\gamma_P}{\gamma_I} \gg 1 \\
\mathrm{Var}\,(r) &\simeq 1 \qquad \text{for } \frac{2\gamma_P}{\gamma_I} \gg 1.
\end{aligned} \tag{6.29}$$

In Figure 10 the mean polarization intensity is shown for $2\gamma_P/\gamma_I = 5$ the graph hardly changes for higher values of the parameter $2\gamma_P/\gamma_I$ and there is only very little difference to the results of the Gaussian approximation [22]. The second-order correlation function $g^{(2)}(0)$ is shown in Figure 11. As in the Gaussian approximation an increase of the second-order correlation function can be seen near threshold. The Gaussian approximation shows however only qualitatively right results, the increase of the photon number fluctuations is much stronger. The decay of the second-order correlation function to Poissonian statistics above threshold cannot be investigated *via* adiabatic elimination because the time-scale separation becomes worse and ceases to exist for $p \gg 1$. This behavior of the photon statistics for a bad-cavity laser with slow inversion near threshold is very different from a good-cavity laser or a bad-cavity laser with slow polarization (see Sect. 6.1) where the correlation function drops from the value $g^{(2)}(0) = 2$ (thermal super-Poissonian statistics) to $g^{(2)}(0) = 1$ (Poissonian statistics) in a narrow neighborhood of the threshold.

7 Power spectrum

The decay of photon-number correlations of the laser mode inside the cavity in steady state is described by the

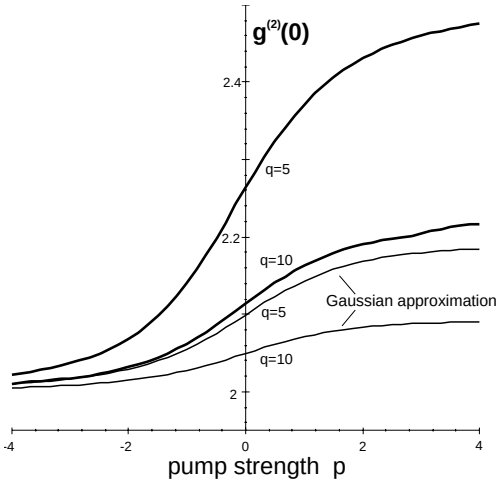

Fig. 11. Second-order correlation function $g^{(2)}(0)$ as a function of the pump strength p for slow inversion ($\alpha \ll 1/10$) for different values of the parameter $q = 2\gamma_P/\gamma_I$. The thin lines give the result of the Gaussian approximation.

time-dependent second-order correlation function

$$g^{(2)}(t) = \frac{\langle b^\dagger(0)b^\dagger(t)b(t)b(0)\rangle}{\langle b^\dagger(0)b(0)\rangle^2}\,. \tag{7.1}$$

For large times $t \gg t_c$ where t_c is the correlation time we have [11]

$$g^{(2)}(t) \longrightarrow 1 \quad \text{for } t \gg t_c. \tag{7.2}$$

The fluctuations of the output field measured outside the cavity are connected to the normalized second-order coherence by

$$\langle I(t)I(0)\rangle = \kappa\langle b^\dagger b\rangle\delta(t) + \kappa^2\langle b^\dagger b\rangle^2 g^{(2)}(t) \tag{7.3}$$

where $\kappa\langle b^\dagger b\rangle\delta(t)$ is the shot-noise contribution. After changing to a Fokker-Planck equation in reduced variables $g^{(2)}(t)$ is calculated by

$$g^{(2)}(\tilde{t}) = \frac{1}{\langle r\rangle^2}\int dr dz\; re^{L_r\tilde{t}}rP_{stat}(r,z) \tag{7.4}$$

where we used rescaled time according to (3.15) $\tilde{t} = (\gamma_I/\alpha)t$. The power spectrum of the intensity fluctuations inside the cavity is defined by the Fourier transform of the second-order coherence

$$S(\omega) = \int dt\, e^{i\omega t}\left(g^{(2)}(t) - 1\right). \tag{7.5}$$

In experiments however the fluctuations of the intensity are measured outside the cavity. The measurable output power spectrum $S^{out}(\omega)$ (defined as Fourier transform of (7.3)) is connected to the intracavity power spectrum by

$$S^{out}(\omega) = S(\omega) + \frac{1}{\kappa\langle b^\dagger b\rangle}\,. \tag{7.6}$$

The difference between inside and outside fluctuations is very important and interesting when dealing with so-called non-classical light (*e.g.* noise reduction under shot-noise level). In the bad-cavity laser described here we may however neglect the difference as $S(\omega)$ will be seen to be strictly positive (so there is no noise reduction in the photon statistics) and typical values of $S(\omega)$ will be large compared to $\dfrac{1}{\kappa\langle b^\dagger b\rangle}$. In fact $S(\omega)$ has the dimension of a time and the typical inverse time scale for $g^{(2)}(t)$ is either γ_I if $\alpha \ll 1$ or γ_I/α if α is of order 1 or larger. Now $\gamma_I S^{out}(\omega) = \gamma_I S(\omega) + \dfrac{1}{\langle r\rangle}\sqrt{\dfrac{8\gamma_I}{n\gamma_P}}$ and $\sqrt{\dfrac{8\gamma_I}{N\gamma_P}} < 10^{-5}$ if $N \sim 10^{10}$. In Figures 12, 13, 14 and 16 some power spectra are plotted and it can be seen that the shot-noise contribution is negligible.

We will calculate the second-order coherence and the power spectrum to show the time-dependent behavior of fluctuations and to show the role of the different time scales involved. In the Gaussian approximation described in Section 4 $g^{(2)}(t)$ and $S(\omega)$ are easily calculated

$$\begin{aligned} g^{(2)}(\tilde{t}) = 1 &+ \frac{1}{r_0(\lambda_+ - \lambda_-)} \\ &\times \left[\left(\langle \Delta r\Delta z\rangle_0 + \frac{\alpha}{\alpha+\lambda_-}\langle\Delta r\rangle_0^2\right)e^{\lambda_+\tilde{t}}\right. \\ &\left. - \left(\langle \Delta r\Delta z\rangle_0 + \frac{\alpha}{\alpha+\lambda_+}\langle\Delta r\rangle_0^2\right)e^{\lambda_-\tilde{t}}\right] \end{aligned} \tag{7.7}$$

where the correlation times $\lambda_\pm$ are given by (5.4). The power spectrum is given by

$$\begin{aligned} S(\omega) = &\frac{\alpha}{\gamma_I\, r_0(\lambda_+ - \lambda_-)} \\ &\times \left[-\left(\langle \Delta r\Delta z\rangle_0 + \frac{\alpha}{\alpha+\lambda_-}\langle\Delta r\rangle_0^2\right)\frac{2\lambda_+}{(\frac{\alpha}{\gamma_I}\omega)^2+\lambda_+^2}\right. \\ &\left. + \left(\langle \Delta r\Delta z\rangle_0 + \frac{\alpha}{\alpha+\lambda_+}\langle\Delta r\rangle_0^2\right)\frac{2\lambda_-}{(\frac{\alpha}{\gamma_I}\omega)^2+\lambda_-^2}\right]. \end{aligned} \tag{7.8}$$

These results for the second-order correlation and the power spectrum are valid above threshold. Near threshold we may again use adiabatic elimination to simplify (7.1) considerably and integrate the remaining Fokker-Planck equation for one degree of freedom numerically. In case of slow polarization the this leads to

$$g^{(2)}(\tilde{t}) = \int dr\; re^{\ell_P\tilde{t}}rP_{stat}(r) \tag{7.9}$$

where ℓ_P is given by (6.9) and $P_{stat}(r)$ by (6.10). In case of slow inversion some care has to be taken as initial slips do occur as described in [17]. As the fast transient is neglected in adiabatic elimination initial conditions have to be shifted to give the right behavior on the slow time scale. A systematic approach to deal with correlation functions of the adiabatically eliminated variables in a Fokker-Planck equation is not known to the author (for initial

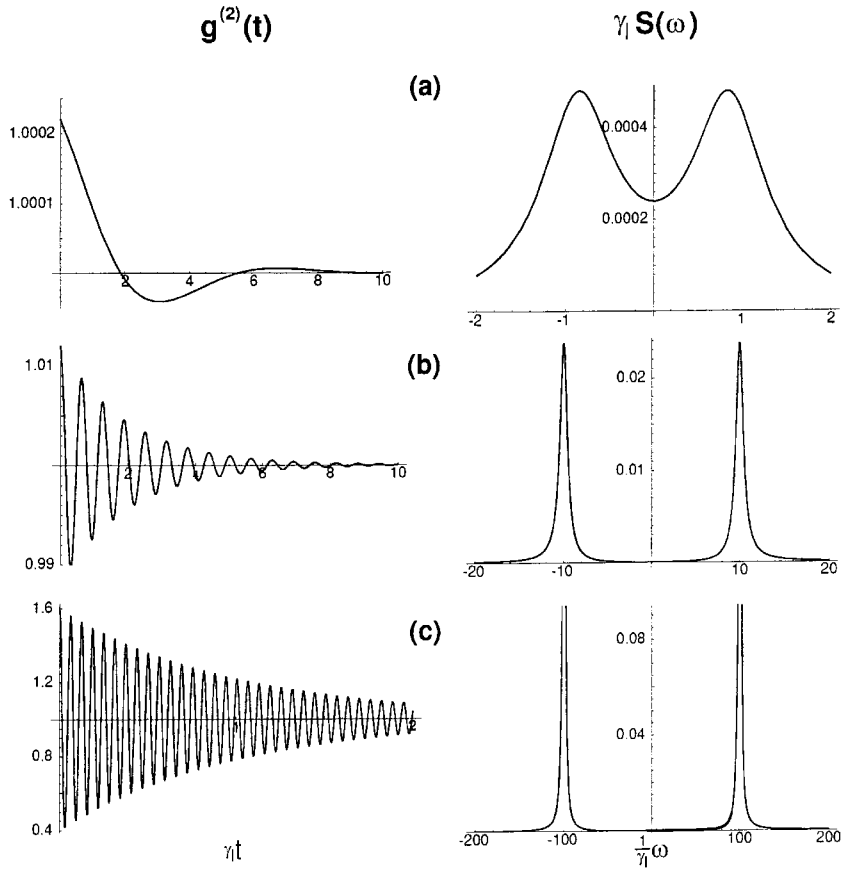

Fig. 12. Second-order correlation function $g^{(2)}(t)$ and power spectrum $S(\omega)$ above threshold in Gaussian approximation: (a) $r_0 \approx p = 100, \alpha = 100, \frac{2\gamma_P}{\gamma_I} = 5$; (b) $r_0 \approx p = 100, \alpha = 1, \frac{2\gamma_P}{\gamma_I} = 5$; (c) $r_0 \approx p = 100, \alpha = 0.01, \frac{2\gamma_P}{\gamma_I} = 5$.

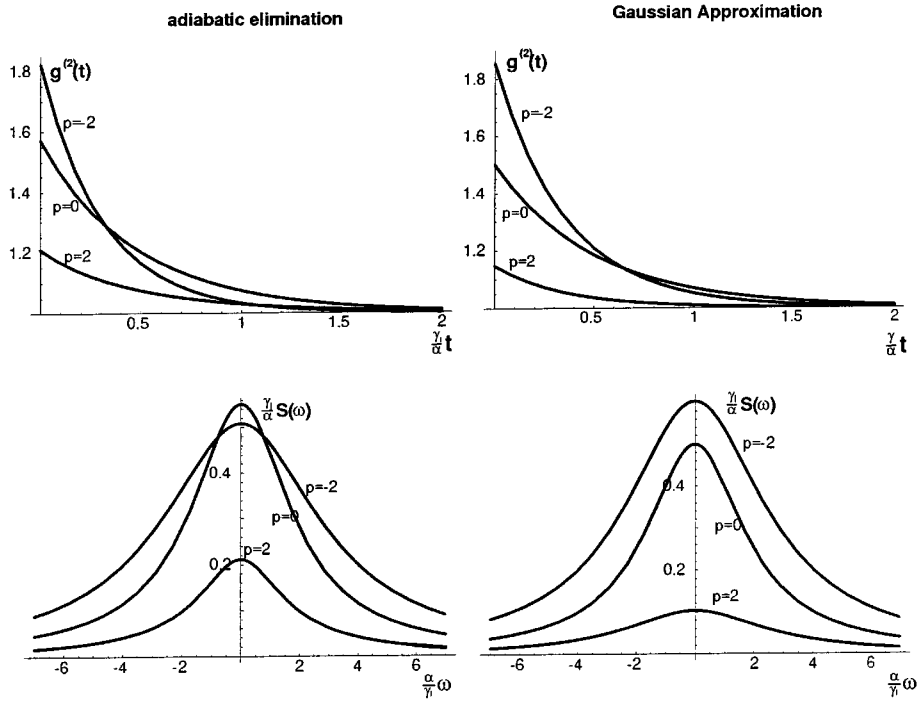

Fig. 13. Slow polarization: second-order correlation function $g^{(2)}(t)$ and power spectrum $S(\omega)$ near threshold in adiabatic elimination and Gaussian approximation ($\alpha = 10000, \frac{2\gamma_P}{\gamma_I} = 5$) for different values of the pump strength p.

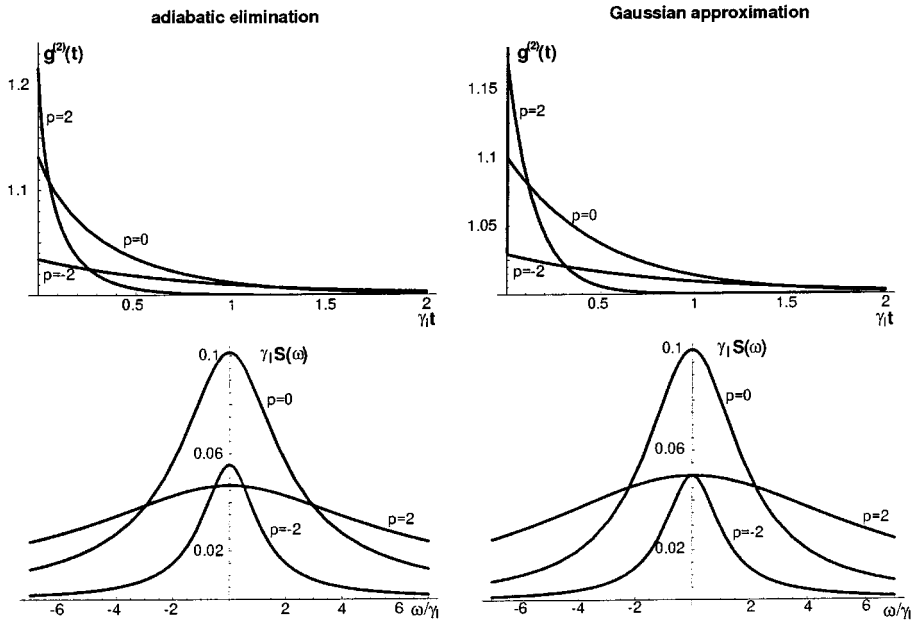

Fig. 14. Slow inversion: second-order correlation function $g^{(2)}(t)$ and power spectrum $S(\omega)$ near threshold in adiabatic elimination and Gaussian approximation ($\alpha = 0.00001$, $\frac{2\gamma_P}{\gamma_I} = 5$) for different values of the pump strength p.

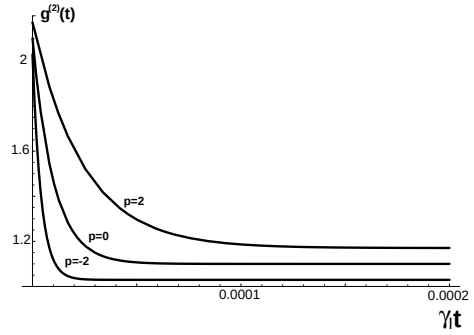

Fig. 15. Slow inversion: second-order correlation function $g^{(2)}(t)$ near threshold Gaussian approximation ($\alpha = 0.00001, 2\gamma_P/\gamma_I = 5$) for different values of the pump strength p and very short time scales.

slips in the reduced probability distribution see [15,17]) but will probably be worked out by the author. As a result $g^{(2)}(0)$ is not the right initial condition for $g^{(2)}(t)$ in case of slow inversion. The right expression to first order is

$$g^{(2)}(\tilde{t}) = \int dz \frac{1}{z}\, e^{\ell_I \tilde{t}}\, \frac{1}{z} P_{stat}(z) \tag{7.10}$$

where ℓ_I is given by (6.22) and $P_{stat}(z)$ by (6.23). A comparison of the Gaussian approximation to the results of adiabatic elimination will clarify this topic of initial slips in the following.

7.1 Power spectrum above threshold

Above threshold where polarization and inversion decay on the same time scale τ_d which is set by the real part of $(\gamma_I/\alpha)\lambda_\pm$

$$\begin{aligned} \tau_d &= -\frac{\alpha}{\gamma_I \Re(\lambda_+)} = \frac{2\alpha r_0}{\gamma_I(1+\alpha r_0)} \\ &\approx \frac{1}{\gamma_I} \qquad \text{for } r_0\,\alpha \gg 1. \end{aligned} \tag{7.11}$$

Oscillations occur in the second-order coherence with a period τ_{osc} determined by the imaginary part of $(\gamma_I/\alpha)\lambda_\pm$

$$\begin{aligned} \tau_{osc} &= 2\pi \frac{2\alpha r_0}{\gamma_I \sqrt{4\alpha r_0^3 - (\alpha r_0 - 1)^2}} \\ &\approx \frac{1}{\gamma_I}\sqrt{\frac{\alpha}{r_0}} \quad \text{for } r_0\,\alpha \gg 1. \end{aligned} \tag{7.12}$$

In Figure 12 the second-order coherence and the power spectrum are plotted for some values of the parameters α and $r_0 \gg 1$. In the power spectrum one sees nicely the peaks at $\omega = 2\pi/\tau_{osc}$ with a width given by $\Delta\omega \approx 1/\tau_d$.

7.2 Power spectrum near threshold

Near threshold the Gaussian approximation becomes inconsistent as the fluctuations $\langle \Delta r \Delta z\rangle_0$, $\langle \Delta r^2\rangle_0$ and $\langle \Delta z^2\rangle_0$ in (4.5) are of the same order as the squared means $r_0 z_0$, r_0^2 and z_0^2 (4.2). Nevertheless the results of Section 7.1 show the same qualitative behavior as the results obtained with adiabatic elimination near threshold.

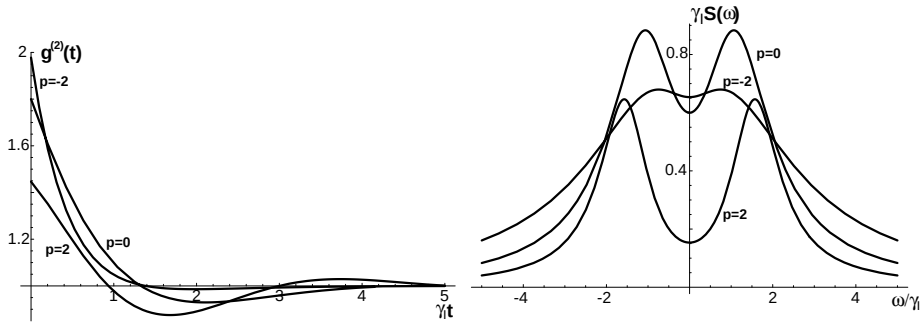

Fig. 16. No time scale separation: second-order correlation function $g^{(2)}(t)$ and power spectrum $S(\omega)$ near threshold in Gaussian approximation ($\alpha = 1, \frac{2\gamma_P}{\gamma_I} = 5$) for different values of the pump strength p.

In Figure 13 the second-order coherence and the power spectrum are shown in the case of slow polarization $\alpha \gg 10$. The plots on the left side are obtained by adiabatic elimination and numerical integration of (7.9) while the plots on the right side show the results (7.7) and (7.8) of the Gaussian approximation. Increasing the pump strength p near threshold leads to less fluctuations on short times while the decay of correlations becomes slower.

For slow inversion $\alpha \ll 0.1$ the plots of both approximations are similar on the slow time scale set by the decay of the inversion as seen in Figure 14. However on very short times of the order of the decay time of the polarization a fast transient is seen in Figure 15 for the second-order coherence function $g^{(2)}(t)$. This transient is neglected in adiabatic elimination leading to an initial slip in the initial condition for $g^{(2)}(t)$.

If there is no time-scale separation near threshold it is not possible to simplify (7.4) systematically. In the regime where adiabatic elimination is possible we have however seen that Gaussian approximation gives a quite good (and much simpler) reproduction of the results obtained more systematically by adiabatic elimination. Assuming that Gaussian approximation captures the main behavior for $\alpha \approx 1$ $S(\omega)$ and $g^{(2)}(t)$ are plotted in Figure 16. The inset of oscillatory behavior is seen as the pump strength is increased.

8 Conclusion

A simple model of a bad-cavity laser has been presented that is based on Haken's master equation for a large number N of incoherently pumped two-level atoms coupled to one mode of a cavity. The bad-cavity limit allows for adiabatic elimination of the mode. Above threshold a Gaussian approximation yields the photon statistics.

Near threshold the remaining atomic dynamics has a further time-scale separation in the cases $\alpha \gg 10$ (slow polarization) and $\alpha \ll 0.1$ (slow inversion). In these cases the slow dynamics is ruled by the decay of the slowest transient and further adiabatic elimination of the fast variable is possible. The remaining dynamics is simple enough to compute the total photon-number distribution of the steady state analytically which is usually a very difficult task in more complex models.

In most lasers $g^{(2)}(0)$ decreases from the value two indicating light from a thermal source to the value one indicating Poissonian statistics as in coherent states as the pump strength is increased near threshold. In contrast to this an increase of $g^{(2)}(0)$ is seen near threshold in the slow-inversion regime $\alpha \ll 0.1$ and only well above threshold there is a slow decrease to the value one as the pumping is increased (see Figs. 3 and 11).

The power spectrum illustrates nicely the different time scales involved in different regimes of the dynamics. If there is no time-scale separation (above threshold or near threshold for $\alpha \approx 1$) the coupled dynamics of polarization and inversion leads to oscillations in the second-order coherence function $g^{(2)}(t)$.

I would like to thank Fritz Haake, Carsten Seeger, Peter Goetsch, Mikhail Kolobov, Robert Graham and J.P. Woerdman for helpful discussions and corrections.

References

1. H. Haken, *Handbuch der Phys.* (Springer, Berlin, 1970)
2. W. Louisell, *Quantum Statistical Properties of Radiation* (Wiley, New York, 1974).
3. M. Sargent III, M.O. Scully, W.E. Lamb Jr., *Laser Phys.* (Addison Wesley, Reading, MA, 1974).
4. W. Weidlich, H. Risken, H. Haken, Z. Phys. **201**, 396 (1967); W. Weidlich, H. Risken, H. Haken, Z. Phys. **204**, 223 (1967); W. Weidlich, H. Risken, H. Haken, Z. Phys. **206**, 355 (1967).
5. M.P. van Exter, S.J.M. Kuppens, J.-P. Woerdman, Phys. Rev. A **51**, 809 (1995); S.J.M. Kuppens, M.P. van Exter, J.-P. Woerdman, Phys. Rev. Lett. **72**, 3815 (1994); J.-P. Woerdman, M.A. van Eijkelenborg, M.P. van Exter, S.J.M. Kuppens, C.A. Schrama, Quant. Semiclass. Opt. **7**, 591 (1995); G. Björk, H. Heitmann, Y. Yamamoto, Phys. Rev. A **47**, 4451 (1993).
6. M.I. Kolobov, L. Davidovich, E. Giacobino, C. Fabre, Phys. Rev. A **47**, 1431 (1993); A.Z. Khoury, M.I. Kolobov, L. Davidovich, Phys. Rev. A **53**, 1120 (1996).

7. L.A. Lugiato, Nuovo Cimento B **50**, 89 (1979); F. Casagrande, L.A. Lugiato, Nuovo Cimento B **55**, 173 (1980); L.A. Lugiato, Lett. Nuovo Cimento **29**, 375 (1980).
8. M.A.M. Marte, P. Zoller, Phys. Rev. A **40**, 5774 (1989); C. Benkert, M.O. Scully, J. Bergou, L. Davidovich, M. Hillery, M. Orszag, Phys. Rev. A **41**, 2756 (1990).
9. Y.M. Golubev, I.V. Sokolov, Zh. Eksp. Teor. Fiz. **87**, 408 (1984) [Sov. Phys. JETP **60**, 234 (1984)]; F. Haake, S.M.Tan, D.F. Walls, Phys. Rev. A **40**, 7121 (1989); T.C. Ralph, C.M. Savage, Phys. Rev. A **44**, 7809 (1991); H. Ritsch, P. Zoller, Phys. Rev. A **45**, 1881 (1992).
10. C.W. Gardiner, *Quantum Noise* (Springer, Berlin, 1991).
11. D.F. Walls, G.S. Milburn, *Quantum Optics* (Springer, 1994).
12. P. Meystre, M. Sargent III, *Elements of Quantum Optics* (Springer, Berlin, 1990).
13. The differences in the generalized Fokker-Planck equation (2.8–2.11) to the form given in [1] is due to a different ordering of the operators in equation (2.7).
14. H. Risken, C. Schmid, W. Weidlich, Z. Phys. **194**, 337 (1966).
15. F. Haake, Z. Phys. B **48**, 31 (1982); F. Haake, M. Lewenstein, Phys. Rev. A **27**, 1013 (1983); F. Haake, M. Lewenstein, Phys. Rev. A **28**, 3606 (1983); F. Haake, M. Lewenstein, Phys. Rev. B **27**, 5868 (1983).
16. N.G. van Kampen, Phys. Rep. **124**, 69 (1985).
17. S. Gnutzmann, F. Haake, Z. Phys. B **101**, 263 (1996).
18. R.J. Glauber, Phys. Rev. **130**, 2529 (1963); R.J. Glauber, Phys. Rev. **131**, 2766 (1963).
19. H. Risken, *The Fokker-Planck Equation*, 2nd edn. (Springer, 1989).
20. A.L. Schawlow, C.H. Townes, Phys. Rev. **112**, 1940 (1958).
21. In experiments done by J.-P. Woerdman the damping and coupling constants are given by

$$\begin{aligned} \kappa &\approx 10^9 \text{ Hz}; \\ \gamma_I &\approx 10^6 \text{ Hz}; \\ \gamma_P &\approx 10^8 \text{ Hz}; \\ g &\approx 10^5 \text{ Hz}; \\ N &\approx 10^{13}. \end{aligned}$$

Thus

$$\alpha \approx 10^{-5}$$

so fast polarization is realized in experiment. J.-P. Woerdman (private communication).
22. The threshold value of the photon number may be calculated from [21] to be $\mathcal{I} \approx 10^4$ or 10^5 whereas in experiment only about 10^3 photons are measured (J.-P. Woerdman, private communication). This difference has its origin in the simplicity of our model which takes into account only two levels of the atom. However in experiment there are losses due to spontaneous decay to other levels.